AEROSPACE RECOMMENDED PRACTICE

ARP6420™

Issued 2021-01

Guidelines for Characterization of Gas Turbine Engine Total-Pressure, Planar-Wave, and Total-Temperature Inlet-Flow Distortion

RATIONALE

The SAE S-16 Turbine Engine Inlet Flow Distortion Committee has developed an Aerospace Recommended Practice (ARP) and Aerospace Information Reports (AIR) describing measurement stations and techniques, and descriptors for different types of inlet total-pressure, planar-wave, and total-temperature distortion. There has been broad acceptance of these descriptors by the industry. Although a treatment for swirl distortion has been proposed, no methodology for swirl distortion has gained wide acceptance. When an accepted methodology exists for swirl distortion, this document will be updated to include it. This document provides a single source that contains the recommended measurement stations and techniques, and descriptors for total-pressure, planar-wave, and total-temperature inlet distortion.

FOREWORD

The most important consideration for successful correlation of data is consistency throughout the ground and flight test programs. Consistency of instrumentation and data reduction techniques should be maintained throughout the test program. The physical layout of the Aerodynamic Interface Plane (AIP), data acquisition, filtering techniques, and data reduction processes should all be agreed upon by all parties (certifying agencies, airframers, engine manufacturers, and ground and flight test organizations) and should be invariant throughout the program. The program should consider the ultimate goals of testing, flow physics, and flow fields being evaluated when designing an air vehicle test program.

NOTICE

This report is published by SAE to advance the state of technical and engineering sciences. The use of this report is entirely voluntary, and its applicability and suitability for any particular use, including any patent infringement arising therefrom, is the sole responsibility of the user. This document has been cleared for public release per Case Number AFLCMC-2020-0192.

TO PLACE A DOCUMENT ORDER: **Tel: 877-606-7323 (inside USA and Canada)**
Tel: +1 724-776-4970 (outside USA)
Fax: 724-776-0790
Email: CustomerService@sae.org
SAE WEB ADDRESS: **http://www.sae.org**

For more information on this standard, visit
https://www.sae.org/standards/content/ARP6420/

TABLE OF CONTENTS

1. SCOPE

The turbine-engine-inlet flow distortion descriptors summarized in this document apply to the effects of inlet total-pressure, planar-wave, and total-temperature distortions. Guidelines on stability margin, destabilizing influences, types and purposes of inlet data, AIP definition, and data acquisition and handling are summarized from AIR5866, AIR5867, ARP1420, and AIR1419. The degree to which these recommendations are applied to a specific program should be consistent with the complexity of the inlet/engine integration. Total-pressure distortion is often the predominant destabilizing element that is encountered and is often the only type of distortion to be considered, i.e, not all types of distortion need to be considered for all vehicles.

2. REFERENCES

2.1 Applicable Documents

The following publications form a part of this document to the extent specified herein. The latest issue of SAE publications shall apply. The applicable issue of other publications shall be the issue in effect on the date of the purchase order. In the event of conflict between the text of this document and references cited herein, the text of this document takes precedence. Nothing in this document, however, supersedes applicable laws and regulations unless a specific exemption has been obtained.

2.1.1 SAE Publications

Available from SAE International, 400 Commonwealth Drive, Warrendale, PA 15096-0001, Tel: 877-606-7323 (inside USA and Canada) or +1 724-776-4970 (outside USA), www.sae.org.

AIR1419 Inlet Total-Pressure-Distortion Considerations for Gas-Turbine Engines

AIR5686 A Methodology for Assessing Inlet Swirl Distortion

AIR5687 Inlet/Engine Compatibility - From Model to Full Scale Development

AIR5866 An Assessment of Planar Waves

AIR5867 Assessment of the Inlet/Engine Temperature Distortion Problem

AIR6345 Processing and Validating CFD Data for Estimating Inlet Dynamic Total-Pressure Distortion

ARP1420 Gas Turbine Engine Inlet Flow Distortion Guidelines

2.1.2 Other Applicable Documents

2.1.2.1 Lytle, J., “The Numerical Propulsion System Simulation: An Overview,” NASA TM-2000-209915, NASA Glenn Research Center, June 2000.

2.1.2.2 Steenken, W., “Planar Wave Stability Margin Loss Methodology,” AIAA 1988-3264, AIAA/ASME/SAE/ASEE 24th Joint Propulsion Conference, Boston, Massachusetts, July 11-13, 1988.

2.1.2.3 “Guide for the Verification and Validation of Computational Fluid Dynamics Simulations,” AIAA G-077-1998.

2.1.2.4 Babcock, D. and Mani, M., “BCFD Predictions of Steady-State and Dynamic Distortion for the 3rd AIAA Propulsion Aerodynamics Workshop,” AIAA 2017-4836, July 2017.

2.1.2.5 Brimelow, B., Collins, T., and Pfefferkorn, G., “Engine Testing in a Dynamic Environment,” AIAA 1974-1198, AIAA/SAE 10th Propulsion Conference, San Diego, CA, Oct. 21-23, 1974.

2.1.2.6 Plourde, G. and Brimelow, B., “Pressure Fluctuations Cause Compressor Instability,” Proceedings of the Air Force Airframe-Propulsion Compatibility Symposium, AD0876608, June 1970.

2.1.2.7 Jacocks, J. and Kneile, K., “Statistical Prediction of Maximum Time-Variant Inlet Distortion Levels,” AEDC-TR-74-121.

2.1.2.8 Tanguy, G., MacManus, D., Garnier, E., and Martin, P., “Characteristics of Unsteady Total-pressure Distortion for a Complex Aero-engine Intake Duct,” Aerospace Science and Technology 78, 2018.

2.1.2.9 Arend, D. and Saunders, J., “An Experimental Evaluation of the Performance of Two Combination Pitot Pressure Probes,”’ NASA TM-2009-215632.

2.2 Definitions

ELEMENT(S): Circumferential- and radial-distortion elements are non-dimensional numerical representations of distortion at the AIP, described on a ring-by-ring basis. There are four fundamental total-pressure-distortion elements defined in ARP1420 including the circumferential distortion intensity (ΔPC/P), circumferential distortion extent (θ^-), circumferential distortion multiple-per-revolution content (MPR), and radial distortion intensity (ΔPR/P). Similar elements are also defined for total-temperature distortion in AIR5867. Other ring-by-ring basis elements can be defined.

DESCRIPTOR(S): Descriptors are non-dimensional numerical representations describing inlet distortion levels at the AIP, using some combination of ring-based distortion elements. There can be any number of distortion descriptors defined including, for example, two-ring or five-ring averages of the circumferential pressure-distortion intensity (ΔPC/P), or two-ring averages of the radial pressure-distortion intensity (ΔPR/P).

CORRELATION(S): Correlations are non-dimensional numerical equations having a unique combination of weighted distortion descriptors. The weightings are empirical sensitivities relating the loss of compression component stability-pressure ratio to inlet distortion. One such example is loss of stability-pressure ratio due to total-pressure distortion, ΔPRS, given by Equation A9 of ARP1420.

2.3 Symbols

C	Constant that relates the root-mean-square of the loss of stability pressure ratio to the maximum loss of stability pressure ratio
C_i	Offset term for ring i (empirically determined)
CT_i	Offset term for ring i (empirically determined)
$C(\tau)$	Covariance
f	Frequency over the range of interest
f_f	Frequency, full scale
f_m	Frequency, model scale
F	Maximum frequency of interest
i	Ring number
j	Rake number
KC_i	Circumferential total-pressure-distortion sensitivity of ring i (empirically determined)
K_{PW}	Component sensitivity to planar waves
KRi	Radial total-pressure-distortion sensitivity of ring i (empirically determined)
KTC_i	Circumferential total-temperature-distortion sensitivity of ring i (empirically determined)

KTR_i	Radial total-temperature-distortion sensitivity of ring i (empirically determined)
L	Characteristic length
l_f	Characteristic length, full scale
l_m	Characteristic length, model scale
MPR_i	Multiple-per-rev element
N	Number of rings
P	Pressure
$\overline{P}$	Mean (time-averaged) total pressure at the AIP
$\widehat{P}_{PEAK}$	Maximum peak-to-peak pressure ratio of planar wave
$\widehat{P}_{RMS}$	Root-mean-square pressure ratio of a planar wave
$\widehat{P}(t_k)$	Non-dimensional time-dependent planar wave at time t_k
PAV_i	Ring i average total pressure
$PAVLOW_i$	Average low total pressure in ring i
$P_i(\theta)$	Function resulting from a linear fit between points of ring i total pressures
PR1	Undistorted flow stability-limit-line total-pressure ratio
PRDS	Distorted flow stability-limit-line total-pressure ratio
PRO	Operating-line total-pressure ratio
R(i)	Radius of ring i
R_{in}	Hub radius
R_{out}	Outer radius
SM	Stability margin
T	Temperature
$T_{0,A,f}$	Ambient air and exhaust gas mixture total temperature at equivalent cross-sections A, full scale
$T_{0,a,f}$	Ambient total temperature, full scale
$T_{0,a,m}$	Ambient total temperature, model scale
$T_{0,e,f}$	Exit total temperature, full scale
$T_{0,e,m}$	Exit total temperature, model scale
$T_{a,f}$	Ambient temperature, full scale
$T_{a,m}$	Ambient temperature, model scale

TAV_i	Ring i average total temperature
$TAVHI_i$	Average high total temperature in ring i
TFAV	Compressor face average temperature
$T(\theta)_i$	Function resulting from a linear fit between points of ring i temperatures
t_f	Time, full scale
t_m	Time, model scale
$U_{a,f}$	Ambient velocity in the axial direction, full scale
$U_{a,m}$	Ambient velocity in the axial direction, model scale
$U_{e,f}$	Exit velocity in the axial direction, full scale
$U_{e,m}$	Exit velocity in the axial direction, model scale
$U_{i,f}$	Inlet velocity in the axial direction, full scale
$U_{i,m}$	Inlet velocity in the axial direction, model scale
$\left(\frac{\Delta PC}{P}\right)_i$	Circumferential total-pressure distortion intensity of ring i
$\left(\frac{\Delta PR}{P}\right)_i$	Radial total-pressure distortion intensity of ring i
ΔPRMS	Change in root-mean-square total pressure
ΔPRS	Loss of stability pressure ratio
ΔSM	Loss of stability margin
$\left(\frac{\Delta TC}{T}\right)_i$	Circumferential total-temperature distortion intensity of ring i
$\left(\frac{\Delta TR}{T}\right)_i$	Radial total-temperature distortion intensity of ring i
θ	Circumferential angle around ring measured from top dead center, degrees
θ^+_i	Circumferential extent of largest region of ring i with temperature above ring i average, degrees
θ^-_i	Circumferential extent of largest region of ring i with pressure below ring i average, degrees
θ^-_{ik}	Circumferential extent of k^{th} region of ring i with pressure below ring i average, degrees
$\rho_{a,f}$	Ambient density, full scale
$\rho_{a,m}$	Ambient density, model scale
$\rho_{e,f}$	Exit density, full scale
$\rho_{e,m}$	Exit density, model scale

τ Lag time, seconds

φ Power spectral density of the waveform formed by the spatial average of the AIP non-dimensional total-pressure waveform at each time step

3. STABILITY MARGIN

Quantitative evaluations of compression-component stability are necessary to provide technical visibility relative to target levels during engine development programs. This is accomplished by using the following definitions to quantify the available stability margin and applicable compression-component destabilizing influences. Test data are required inputs to the stability margin calculations.

The available stability margin for a specific compression component at a given corrected airflow is defined as the difference between the clean-inlet-flow stability-limit-line total-pressure ratio and the operating-line total-pressure ratio non-dimensionalized by the operating line total-pressure ratio. In numerical terms with reference to Figure 1:

$$SM = \left(\frac{PR1-PRO}{PRO}\right) \times 100 \quad \text{(Eq. 1)}$$

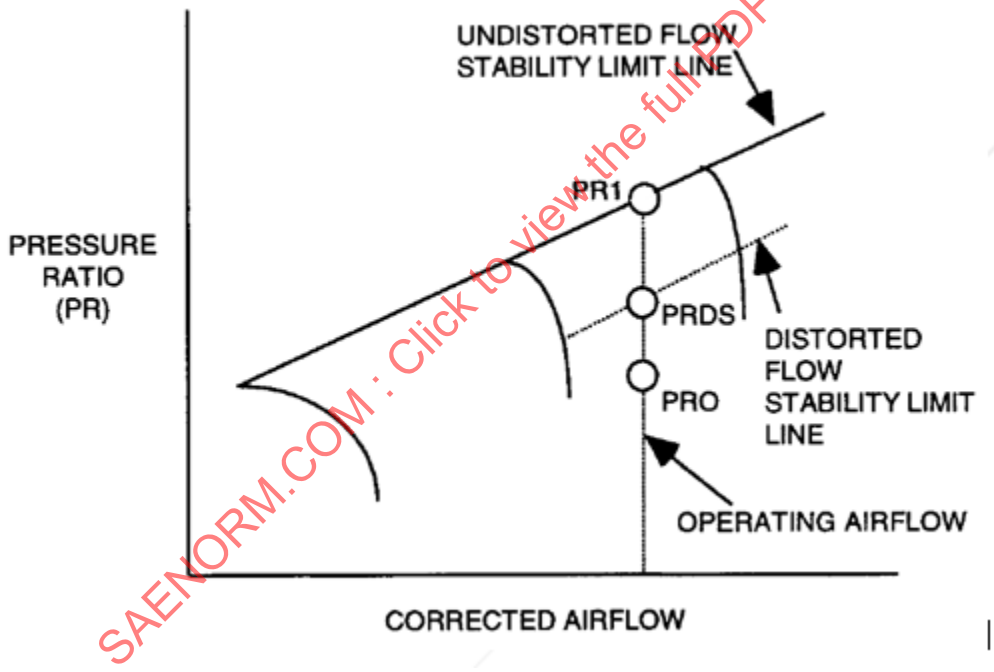

Figure 1 - ARP1420 stability margin definition

The loss of stability pressure ratio is defined as the decrease in total-pressure ratio relative to the stability-limit-line total-pressure ratio non-dimensionalized by the stability-limit-line total-pressure ratio, all at constant corrected airflow. Numerically and with reference to Figure 1, it is defined as:

$$\Delta PRS = \left(\frac{PR1-PRDS}{PR1}\right) \times 100 \quad \text{(Eq. 2)}$$

The loss in stability pressure ratio as it relates to available stability margin is defined as the decrease in total-pressure ratio relative to the undistorted stability limit line total-pressure ratio non-dimensionalized by the operating line total-pressure ratio, all at constant corrected airflow. Numerically and with reference to Figure 1, it is defined as:

$$\Delta SM = \left(\frac{PR1-PRDS}{PRO}\right) \times 100 \quad \text{(Eq. 3)}$$

4. STABILITY ASSESSMENTS

Assessments should be carried out regularly and in increasing detail throughout the development and life cycles of a propulsion system. A stability assessment provides quantitative estimates of the effects of inlet distortion and other destabilizing influences on compression-component stability. The assessment should be performed in a manner to reveal the stability margin usage by accounting for the factors that lower the compression-component stability limit line and/or raise the compression-component operating line. The assessment, performed at constant corrected engine airflow (the matched inlet-engine corrected airflow at the steady-state operating point corresponding to the propulsion-system operating condition being investigated), requires that compression-component stability limit lines be defined over the entire corrected-airflow operating range for each compression component.

Factors to be considered, if appropriate, include external destabilizing factors and internal destabilizing factors. External destabilizing factors can include but are not limited to time-variant inlet total-pressure distortion, planar waves (in-phase total-pressure oscillations), time-variant inlet total-temperature distortion, inlet swirl distortion, and exit static-pressure distortion. Internal destabilizing factors can include but are not limited to component interactions, deterioration, component variation due to manufacturing tolerances, control tolerances, variable-geometry position, power-lever transients, operating-point shift with distortion, Reynolds number effects, compression component bleed, intra-compression component bleed, and horsepower extraction.

The effect of each factor is expressed as a change in stability margin. The loss in stability margin for the external destabilizing factors is computed from the distortion-descriptor elements and their respective sensitivities, which are then combined for each type of distortion. Some effects of factors are cumulative and should be added algebraically, whereas other effects of factors are random and should be added statistically (ARP1420, AIR1419). The method and rationale for combining individual effects should be delineated and supported by test experience.

Total-pressure distortion transfer coefficients and total-temperature generation coefficients are used to transfer inlet-distortion effects to the downstream compression components. Stability assessments are made for each compression component.

Stability assessments should be conducted at the Mach numbers, altitudes, airflows, and engine operating and maneuver conditions (angles of attack and sideslip) necessary for performance and operability verification, including the appropriate inlet recovery and the effects of any compression-component rematch.

5. TESTING

Testing during propulsion system development and throughout the vehicle life cycle may be required to develop and verify stability and performance assessments. The validity of the assessments depends on the quality of the data generated during the testing effort.

5.1 Test Planning

A master test plan should be developed early in the program. This test program, which defines test techniques, instrumentation, data management, test equipment and procedures, and the analysis and communication of test results, should be agreed upon by all involved parties.

5.1.1 Testing Scope

Tests that may be required prior to production will depend on the propulsion system under development. The types of test and test objectives follow.

5.1.2 Inlet and Aircraft Component Tests

These tests include scale-model inlet/forebody tests, control bench tests, and full-scale or large-model tests with inlet control. The objective of these tests is to provide data for inlet development, distortion level and pattern definition, off-schedule geometry and bleed effects, inlet stable flow range, and definition of control system/inlet destabilizing effects.

5.1.3 Engine and Engine Component Tests

These consist of compressor, diffuser, control, burner, augmentor, fuel system, and engine tests, with and without inlet pressure distortion. The objective of the tests is to provide data for distortion-descriptor development, control and sensor development, scheduled and off-schedule geometry, bleed effects, Reynolds number effects, component interactions, engine performance, and stability evaluation. Stability data should be obtained whenever practical.

5.1.4 Propulsion System Tests

These tests consist of static, simulated altitude, and flight tests. The objectives of the tests are to evaluate propulsion system stability, system operational characteristics, failure modes, and control interactions throughout the flight and maneuver envelopes.

5.2 Stability and Performance Tests

Tests should be conducted at environmental conditions representative of projected mission-related flight conditions. Inlet and engine operating conditions must be defined and should include the following:

a. Inlet: Inlet configuration details, mass flow ratio, corrected airflow, Reynolds number, Mach number, aircraft angles of attack and sideslip, and bleed flows

b. Engine: Engine configuration details, operating corrected speeds, corrected airflow, bleed flows, power extraction requirements, control function (steady-state or transient), operating mode (afterburning, non-afterburning, etc.), compressor-face total pressure and total temperature, and compressor inlet total-pressure distortion pattern (probe values)

Engine tests provide data for verification of stability assessment line items, stability audit methodology at critical flight points, stability demonstration, and documentation. Compressor stability-limit-line and stability-margin utilization data together with compressor speed, compressor airflow, and efficiency changes are obtained from tests on representative components.

During stability testing, engine operation in the region above the maximum predicted operating line and below the predicted stability pressure ratio should be accomplished whenever practical. Stability data for the stability assessment can be obtained by use of compressor loading techniques that account for engine control logic and mechanical limitations. Documentation should include operating-line excursions caused by the primary stability degrading factors such as inlet distortion and control requirements. The compressor stability margin utilization estimated for engine aging factors such as deterioration should be verified on the basis of life-cycle and/or service engine tests of production engines.

If distortion effects are demonstrated to have a strong effect on thrust, then the sensitivity must be determined.

6. TYPES OF DISTORTION

In the following subsections, the equations for the distortion elements for total-pressure, planar-wave, and total-temperature distortions are provided. The total-pressure, planar-wave, and total-temperature distortion elements are developed from measurements made using a ring-rake array located at the AIP (see Section 7).

6.1 Total-Pressure Distortion

The equations and figures defining the total-pressure distortion elements are described in the sections below. Additional information about total-pressure distortion can be found in ARP1420 and AIR1419.

Total-pressure distortion can be described as a spatial variation in total pressure at the AIP. There are both steady-state and time-variant (dynamic) components of total-pressure distortion. Steady-state total-pressure distortion is the spatial variation in time-averaged total pressure across the AIP. Time-variant total-pressure distortion is determined from measurements of total pressure using high-response pressure sensors located at a number of locations at the AIP. The peak distortion pattern that is present for a time period that could cause a destabilizing engine response, typically on the order of one-half to one rotor revolution, represents the peak, e.g., destabilizing, total-pressure distortion.

6.1.1 Stability Pressure-Ratio-Loss Correlation

The loss of stability pressure ratio due to total-pressure distortion, expressed as a percent of the undistorted stability pressure ratio, is determined using the distortion correlation, ΔPRS, as expressed in Equation 4. Total-pressure distortion is described in terms of circumferential and radial distortion elements.

$$\Delta PRS = \sum_{i=1}^{N} \left[KC_i \times \left(\frac{\Delta PC}{P}\right)_i + KR_i \times \left(\frac{\Delta PR}{P}\right)_i + C_i \right] \times 100 \quad \text{(Eq. 4)}$$

where the distortion elements are:

N = number of instrumentation rings

KC_i = circumferential total-pressure distortion sensitivity of ring i (empirically determined)

KR_i = radial total-pressure distortion sensitivity of ring i (empirically determined)

$(\Delta PC/P)_i$ = circumferential total-pressure distortion intensity of ring i defined in Equation 6

$(\Delta PR/P)_i$ = radial total-pressure distortion intensity of ring i defined in Equation 16

C_i = offset term for ring i (empirically determined)

6.1.2 Total-Pressure Distortion Elements

The equations and figures defining the total-pressure distortion elements appear in the sections below.

The Aerodynamic Interface Plane (AIP, defined and described in Section 7) total-pressure probe data are used to describe inlet total-pressure distortion directly in terms of the instantaneous total-pressure contours (pattern) and numerically in terms of distortion descriptors that are related to the severity of the distortion. Distortion descriptors provide a means of identifying critical distorted inlet-flow conditions and of communicating during propulsion system development and life cycles. Distortion elements have been identified for use in creating a distortion sensitivity correlation for a particular engine. These elements are combined to define each distortion descriptor system. The distortion elements are used to quantify the distortion at the AIP. Fundamental to the distortion elements is the set of total pressures that are used to describe the total-pressure distribution. The total-pressure probes usually are arranged in rake and ring arrays. Circumferential- and radial-distortion elements, which are calculated using the total-pressure probe measurements, are defined on a ring-by-ring basis. Inlet spatial distortion is described in terms of circumferential and radial elements and is discussed in detail in the following paragraphs.

Circumferential distortion is described for each instrumentation ring in terms of intensity, extent, and multiple-per-revolution elements.

a. Intensity: The circumferential distortion intensity element (ΔPC/P) is a numerical indication of the magnitude of the total-pressure defect for each ring.

b. Extent: The circumferential distortion extent element (θ^{-}) is the angular region, in degrees, in which the total pressure is below the ring-average total pressure.

c. Multiple-per-Revolution: The circumferential distortion multiple-per-revolution element (MPR) is a numerical indication of the “effective” number of low total-pressure extents for each ring.

The radial-distortion intensity element (ΔPR/P) describes the difference between the ring-average total pressure and the face-average total pressure for each ring. Both positive and negative values of radial intensity are possible. Positive values reflect a ring-average total pressure that is below the face-average total pressure.

6.1.3 Distortion Elements for Total-Pressure Distortion

The numerical calculations of the distortion elements are summarized in this section. These elements are used in determining the stability margin for an engine. More information about total-pressure distortion can be found in ARP1420 and AIR1419.

6.1.3.1 Circumferential Distortion Elements

As described in 6.1.2, circumferential distortion is calculated on a ring-by-ring basis in terms of intensity, extent, and multiple-per-revolution elements. The intensity or level of distortion is a numerical indication of the magnitude of the total-pressure distortion. The extent element is a numerical indication of the circumferential size of the low total-pressure region. The multiple-per-revolution element is a numerical indication of the equivalent number of circumferential regions of low total-pressure.

6.1.3.1.1 One-Per-Rev Patterns

The “intensity” and “extent” elements of circumferential distortion are obtained by linear interpolation of the total pressures in a given instrumentation ring. An example of total pressures for the probes in the i^{th} ring for a one-per-revolution pattern (one total-pressure defect in 360 degrees) is shown in Figure 2. Theta minus, θ_i^-, is the circumferential extent of the low total-pressure region. It is defined by the intersection between the ring average total pressure and the linear interpolation which subtends the low total-pressure extent (θ_2 - θ_1).

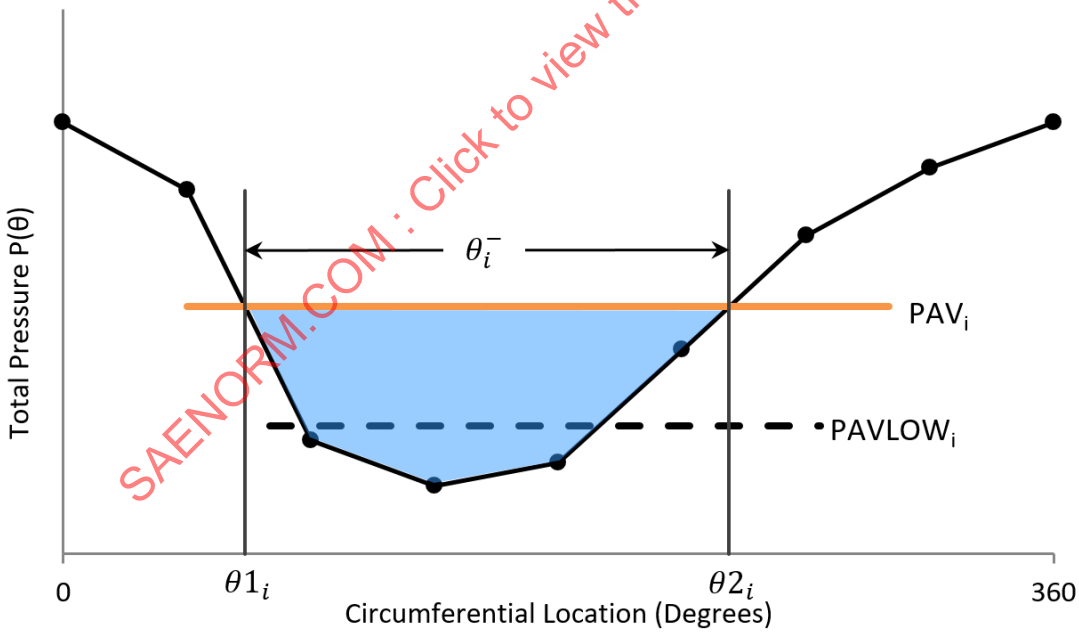

Figure 2 - Ring circumferential distortion for a one-per-rev pattern

$$\text{Extent: } \theta_i^- = \theta_{2i} - \theta_{1i} \qquad \text{(Eq. 5)}$$

$$\text{Intensity: } \left(\frac{\Delta PC}{P}\right)_i = \left(\frac{PAV - PAVLOW}{PAV}\right)_i \qquad \text{(Eq. 6)}$$

where:

$$PAV_i = \frac{1}{360}\int_0^{360} P_i(\theta)\, d\theta \quad \text{(ring i average total pressure)} \qquad \text{(Eq. 7)}$$

$P_i(\theta)$ is a function resulting from a linear fit between the data points of ring i.

$$PAVLOW_i = \frac{1}{\theta_i^-}\int_{\theta_{1_i}}^{\theta_{2_i}} P_i(\theta)\, d\theta \quad \text{(average low total pressure in ring i)} \qquad \text{(Eq. 8)}$$

Because this is a one-per-rev pattern, the multiple-per-rev distortion element is defined as:

$$\text{Multiple-Per-Rev: } MPR_i = 1 \qquad \text{(Eq. 9)}$$

6.1.3.1.2 Multiple-Per-Rev Patterns

The circumferential distortion intensity extent elements for multiple-per-revolution distortion patterns are also determined by a linear interpolation procedure. A pattern with two low total-pressure regions relative to the ring average separated by two high total-pressure regions of extents θ_{i1}^+ and θ_{i2}^+ is shown in Figure 3. In all that follows, the analytical expressions will be written for the k-th low-total-pressure region for Q low-total-pressure regions per ring. The intensity and extent elements of each low-total-pressure region are calculated using Equations 5 and 6.

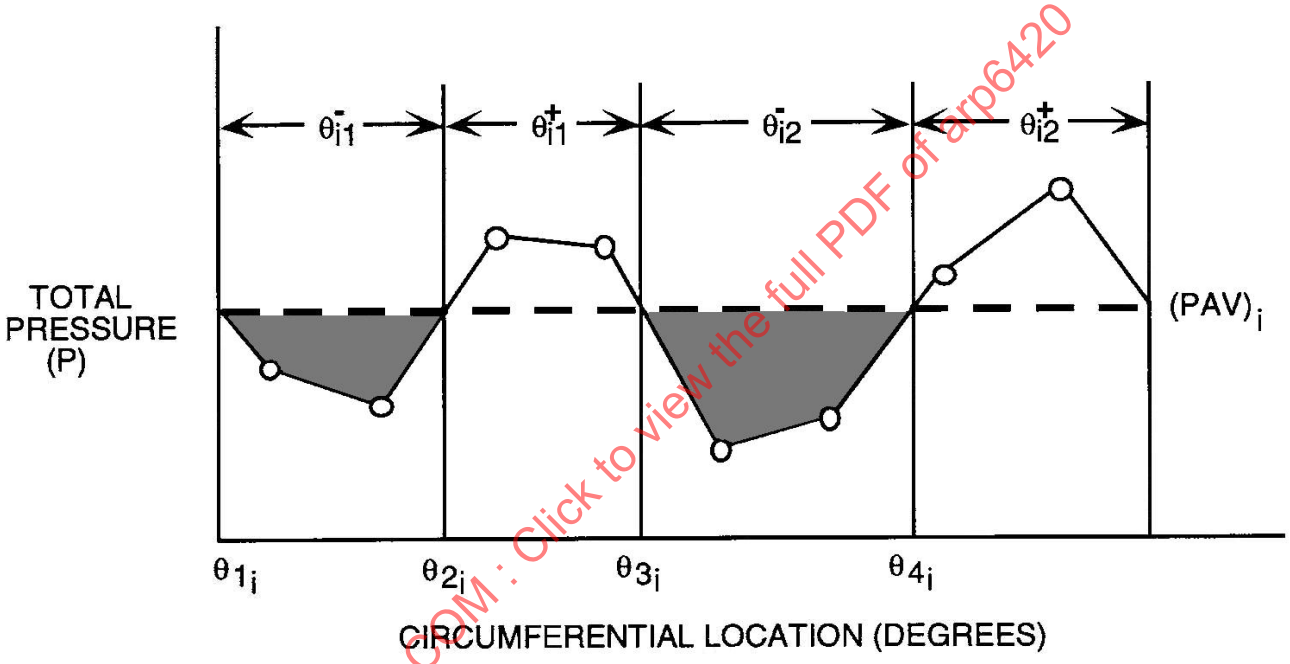

Figure 3 - Ring circumferential distortion for a multiple-per-rev pattern

6.1.3.1.2.1 Patterns with $\theta_{ik}^+ \leq \theta_{min}^+$

If the pattern has low total-pressure regions circumferentially separated by high total-pressure regions with extents less than or equal to θ_{min}^+, it is considered as an equivalent one-per-revolution low total-pressure region and the multiple-per-revolution element is 1.0. θ_{min}^+ is specified by the descriptor system developer. A value of θ_{min}^+ of 25 degrees is suggested in the absence of other information.

$$\text{Extent: } \theta_i^- = \sum_{k=1}^{Q} \theta_{ik}^- \qquad \text{(Eq. 10)}$$

From Figure 3, $\theta_i^- = (\theta_2 - \theta_1)_i + (\theta_4 - \theta_3)_i$:

$$\text{Intensity: } \left(\frac{\Delta PC}{P}\right)_i = \left(\frac{PAV - PAVLOW}{PAV}\right)_i \qquad \text{(Eq. 11)}$$

where:

$$PAVLOW_i = \frac{1}{\theta_i^-}\sum_{k=1}^{Q}\int_{\theta_{ik}^-} P(\theta)_i \, d\theta \quad \text{(Eq. 12)}$$

Hence,

$$\text{Intensity: } \left(\frac{\Delta PC}{P}\right)_i = \frac{\sum_{k=1}^{Q}\left[\left(\frac{\Delta PC}{P}\right)_{ik}\theta_{ik}^-\right]}{\sum_{k=1}^{Q}\theta_{ik}^-} \quad \text{(Eq. 13)}$$

$$\text{Multiple-Per-Rev: MPR = 1} \quad \text{(Eq. 14)}$$

6.1.3.1.2.2 Patterns with $\theta_{ik}^+ > \theta_{min}^+$

If the pattern has low-total-pressure regions circumferentially separated by high-total-pressure regions with extents greater than θ_{min}^+ then the multiple-per-revolution element is greater than one.

Intensity $\left(\frac{\Delta PC}{P}\right)_i$ is the $\left(\frac{\Delta PC}{P}\right)_{ik}$ corresponding to the maximum value of $\left[\left(\frac{\Delta PC}{P}\right)_{ik}\theta_{ik}^-\right]$.

Extent: θ_i^- is the θ_{ik}^- corresponding to the maximum value of $\left[\left(\frac{\Delta PC}{P}\right)_{ik}\theta_{ik}^-\right]$.

The multiple-per-revolution term is defined as the number of equivalent low-total-pressure regions, the equivalence being based on the ratio of the total integrated area beneath PAV_i in Figure 3 to the largest single area beneath PAV_i. This is given by the equation:

$$\text{Multiple-Per-Rev: } MPR_i = \frac{\sum_{k=1}^{Q}\left[\left(\frac{\Delta PC}{P}\right)_{ik}\theta_{ik}^-\right]}{max\left[\left(\frac{\Delta PC}{P}\right)_{ik}\theta_{ik}^-\right]} \quad \text{(Eq. 15)}$$

6.1.3.2 Radial Distortion Elements

The radial distortion intensity of a ring is defined as the difference between the face-average total pressure and the ring-average total pressure, divided by the face-average total pressure. Both positive and negative values of radial intensity are considered; positive values reflect a ring average total pressure that is below the face average. A tip-radial distortion pattern is illustrated in Figure 4. The arrows indicate the difference in radial total pressure for ring 5. For the general ring, i, the radial intensity is given as:

$$\text{Intensity: } \left(\frac{\Delta PR}{P}\right)_i = \frac{PFAV - PAV_i}{PFAV} \quad \text{(Eq. 16)}$$

where PFAV is the area-weighted average total pressure:

$$PFAV = \frac{1}{N}\sum_{i=1}^{N} PAV_i \quad \text{(Eq. 17)}$$

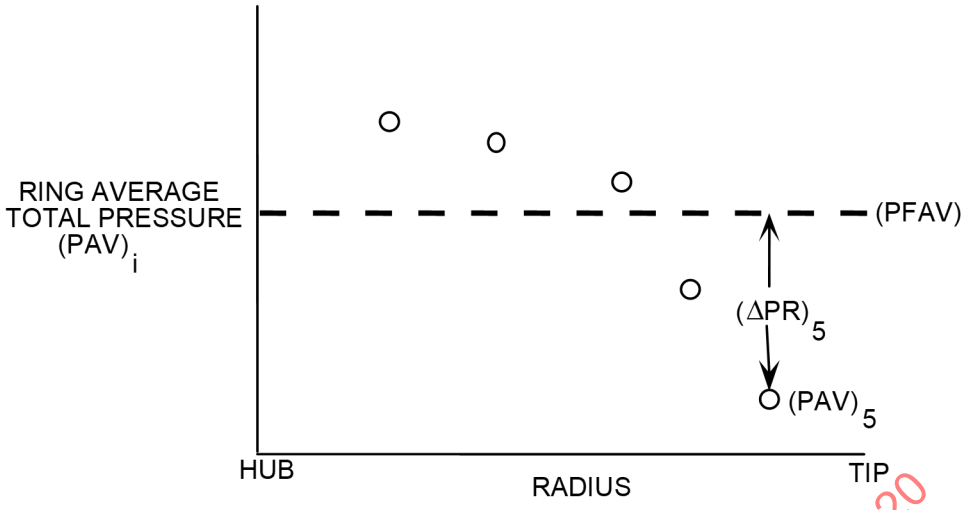

Figure 4 - Radial distortion pattern

6.2 Planar Waves

The equations defining planar waves, methods of addressing the presence of planar waves (avoidance or stability accounting for planar waves), and the categorization of types of planar waves are described in the sections below. Additional information can be found in AIR5866.

Planar waves are time-variant one-dimensional changes in full engine-face total pressure. Reported sources of planar waves include both inlet-generated and externally-generated disturbances. The inlet-generated disturbances include boundary layer separation, shock/boundary layer interactions, supersonic flight buzz/unstart, interactions with adjacent inlet/engines, instabilities during subsonic and supersonic flight at low mass flows, and supersonic-inlet response to inlet control system inputs. Externally-generated total-pressure oscillations include vortices and wakes from nose gear, nose booms, antennas, bomb bay doors, and other external geometry features (protuberances). Background information can be found in AIR1419. Additional supporting information can be found in AIR5866.

6.2.1 Definition of Planar Waves

Planar waves are defined by the manner in which all the AIP total-pressure probes (see 7.1 for the recommended ring-rake array for the total-pressure probes) respond relative to the time-averaged total pressure. The individual pressures are first filtered to a frequency specified by the engine manufacturer, typically commensurate with one-half- to one-per-rev at 100% speed of the engine. The time-variant planar wave is defined as the variation of the face-average time-variant total pressure about the mean steady-state total pressure at the AIP.

In equation form, the mean (time-averaged) total pressure at the AIP is defined as:

$$\bar{P} = \frac{1}{M}\sum_{k=1}^{M}\left[\frac{1}{N}\sum_{i=1}^{N} P_i(t_k)\right] \qquad \text{(Eq. 18)}$$

where:

$P_i(t_k)$ = the total pressure at the i-th probe for the k-th time step

M = number of time steps in the total-pressure sample

N = the number of working and/or substituted total-pressure probes at the AIP

Then, the non-dimensional time-dependent planar-wave total-pressure ratio at time k is defined as:

$$\hat{P}(t_k) = \frac{1}{N}\sum_{i=1}^{N}\left\{\frac{[P_i(t_k)-\bar{P}]}{\bar{P}}\right\} \quad \text{(Eq. 19)}$$

This operation “averages out” much of the random content at the AIP and leaves the non-random content – the planar wave.

The planar wave content for a test or flight condition is expressed as a numerical value, typically as a maximum peak-to-peak value or a root-mean-square (rms) value of the waveform taken over the M time steps of the total-pressure samples. Limiting values will be defined by the engine manufacturer.

The root-mean-square value of the planar-wave pressure is defined as:

$$\hat{P}_{RMS} = \sqrt{\frac{1}{M}\sum_{k=1}^{M}\left[\hat{P}(t_k) - 1\right]^2} \quad \text{(Eq. 20)}$$

The inlet airframe community uses a parameter usually called “SUM40” which often is monitored during inlet tests. This parameter is equivalent to $\hat{P}_{RMS}$. The engine manufacturer is responsible for supplying the limiting value of this parameter. In the absence of a supplied value, 1.5% is often used as the limiting value.

In the case of the maximum peak-to-peak value, the definition provided by the engine manufacturer will address whether it is defined using adjacent maximum and minimum waveform values or the maximum and the minimum from the whole sample.

If the planar wave is sinusoidal or near sinusoidal, then the relationship of the rms to the peak is straightforward.

$$\hat{P}_{PEAK} = \frac{1}{0.707}\hat{P}_{RMS} \quad \text{(Eq. 21)}$$

6.2.2 Methodologies for Addressing Planar Waves Exceeding Limits

When the peak values of the planar wave exceed the limit provided by the engine manufacturer, planar waves are addressed in one of two ways: (1) avoidance or (2) estimating the loss of stability pressure ratio. These are described in the sections below.

6.2.2.1 Avoidance of Planar Waves

Avoidance of the impact of planar waves beyond the level prescribed by the engine manufacturer is usually addressed by the airframer modifying the design of the inlet system to lower the level of planar waves to an acceptable level. Once the airframer has exhausted use of design changes and the level of planar waves at flows within the engine airflow operating range at a given Mach number still exceeds the allowable limit, then it may be possible for the engine manufacturer to raise the “idle airflow lockup” schedule assuming that the idle airflow remains low enough that the airframer can meet aircraft decel requirements.

Thus, the preferred method of addressing planar waves is for the airframe and engine manufacturers to work together to find a workable method that keeps the magnitude of the planar wave below the limit defined by the engine manufacturer. If the planar wave values still exceed the limits provided by the engine manufacturer, then estimates of the loss of stability pressure ratio due to planar waves must be made and included as a line item in stability assessments.

6.2.2.2 Estimating the Loss of Stability Pressure Ratio Due to Planar Waves

Estimating the loss of stability pressure ratio due to planar waves requires addressing the effects on both the stability limit line and the operating line. The manner in which estimates of the loss of stability pressure ratio are made is often dictated by the nature of the planar waves and the manner in which the sensitivities to planar wave were (or are) derived.

6.2.2.2.1 Categories of Planar Waves

The categorization of planar waves requires examination of the planar waveform using power spectral density (PSD) analysis. Inlet-produced planar waves typically fall into one of four categories as follows:

a. Sinusoidal: The PSD of face-average total-pressure recovery shows that all energy is predominately at one specific frequency. Inlet buzz and subsonic low-airflow instability are typical sources of this type of planar wave.

b. Periodic: The PSD of face-average total-pressure recovery shows that energy of the wave occurs at several specific frequencies. Inlet low-flow instability is a typical source of this type of planar wave.

c. Random: The PSD of face-average total-pressure recovery shows that energy of the wave is distributed over a broad range of frequencies. Armaments and weapons bay doors are typical sources for these types of planar waves.

d. Random plus harmonic: The PSD shows a distribution of energy over a broad range of frequencies, punctuated by peaks of energy at one or more frequencies. Nose landing gear can produce this type of planar wave.

Examples of the waveforms and the associated power-spectral densities are illustrated schematically in Figure 5.

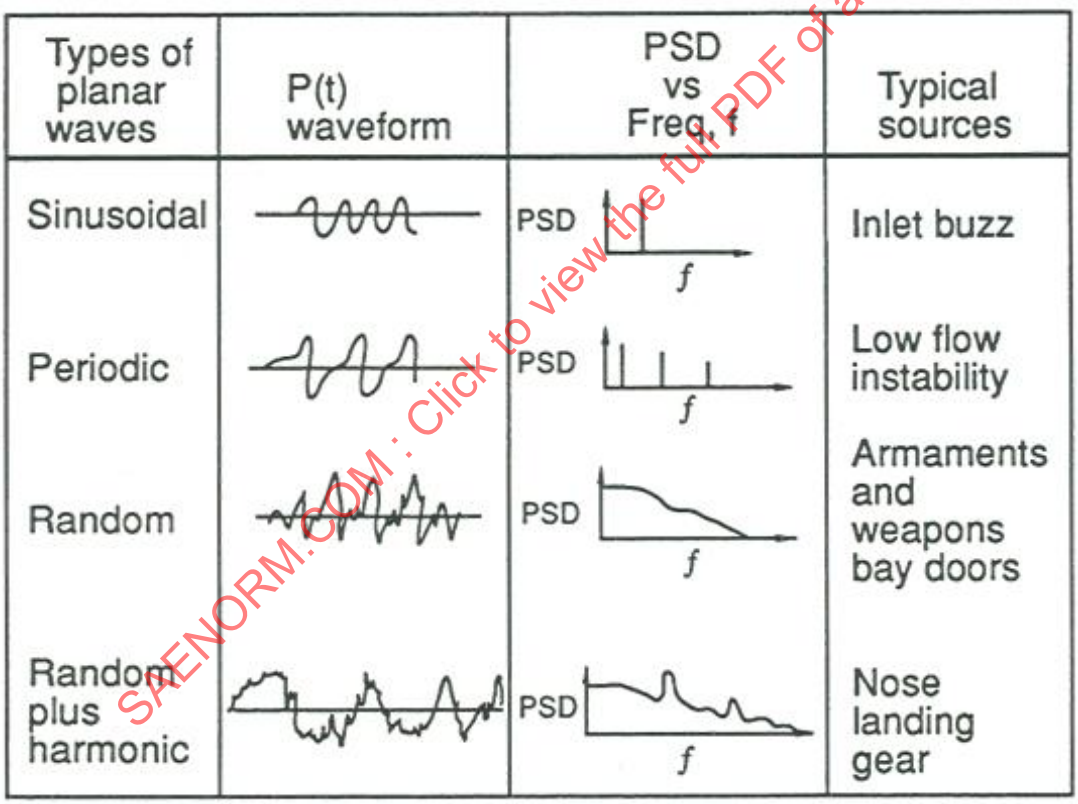

Figure 5 - Categorization of planar waves in inlets

6.2.2.2.2 Estimating Loss of Stability Pressure Ratio for Engines or Compression Components

The sensitivity of engines or compression components to planar waves can be obtained from engine tests, component tests, and/or some combination of engine-transient-cycle models and higher-fidelity compression-component models that will represent the impact of planar waves on the operating line and on the stability limit line of a compression component.

If an engine is subjected to planar waves of the frequency expected in flight, then the phasing between the impacts on the stability limit line and the operating line is inherent in the resulting test data. The stability-limit-line sensitivity to planar waves can extend to frequencies commensurate with the 50% to 100% 1/rev speed of the engine while the impact of planar waves on the operating line is mainly through the fuel control, which can respond to sensor inputs only up to approximately 20 Hz.

The sensitivity of compression components to planar waves requires addressing both the stability-limit-line and the operating-line effects separately. Tests have been defined for obtaining stability-limit-line effects (AIR1419). The operating-line effects can be estimated using the engine-transient-cycle model with the measured planar waveform as input (Reference 2.1.2.1).

The key to making robust estimates of stability-limit-line loss of stability pressure ratio is to know the manner in which the sensitivity to planar waves was derived or is being reported, i.e., whether it is based on peak-to-peak amplitude, rms amplitude, or the sinusoidal amplitude (sometimes inaccurately referred to as half amplitude).

The following information can be of help when trying to derive planar-wave sensitivities with any of the above categories of planar wave.

6.2.2.2.3 Estimating the Loss of Stability Pressure Ratio

The loss of stability pressure ratio due to planar waves, in its most general form, can be represented by the following expression:

$$\Delta PRS = C\sqrt{\int_0^F [K_{PW}(f)]^2\ \phi\ df} \qquad \text{(Eq. 22)}$$

where:

C = constant that relates the root-mean-square of the loss of stability pressure ratio to the maximum loss of stability pressure ratio

F = the maximum frequency of interest, typically up to the 1/rev speed of the compression component

f = frequency within the range of interest (0 to F)

K_{PW} = component sensitivity to planar waves and is a function of frequency

ϕ = power spectral density of the waveform formed by the spatial average of the AIP non-dimensional total-pressure waveform at each time step

If only a single frequency is present, then the sensitivity K_{PW} is a constant and the above equation becomes:

$$\Delta PRS = C\ K_{PW}\sqrt{\int_0^F \phi\ df} = C\ K_{PW}\ \hat{P}_{RMS} \qquad \text{(Eq. 23)}$$

where:

$\hat{P}_{RMS}$ = root-mean-square of the AIP non-dimensional total-pressure waveform about its mean value

If the waveform is a true sinusoid, then C equals 1/0.707.

The planar-wave category will dictate whether Equation 22 or Equation 23 should be used.

An example of applying this type of analysis can be found in Reference 2.1.2.2.

6.3 Total-Temperature Distortion

The equations and figures defining the total-temperature distortion elements are described in the sections below. Additional information about total-temperature distortion can be found in AIR5867.

Total-temperature distortion can be described as a spatial variation in total temperature at the AIP and/or a rapid change in the total-temperature average at the AIP. It is important to define a practical face-average total temperature to act as a base for determining distortion descriptors. Since engine power is a function of a change of enthalpy and slow total-temperature changes can affect the compression-system mechanical speeds and matching, the enthalpy-mean total temperature is the technical preference. Test results have shown that the area-weighted definition is very close to the enthalpy-mean definition. Total temperature is related to stagnation enthalpy via air mass flow. In a highly distorted inlet, it is difficult to determine the local airflow in order to calculate the enthalpy distribution. Consequently, the S-16 Committee recommends the area-weighted definition of face-average total temperature.

Total temperatures at the AIP vary with time. The engine can respond to total-temperature fluctuations at frequencies corresponding to the full-scale engine rotation speed. However, the frequency response characteristics of sufficiently-robust total-temperature instrumentation currently available is well below that frequency. To obtain an estimate of the true time-variant total temperature, observed total-temperature readings must be corrected for probe recovery factor and lag.

6.3.1 Stability Pressure-Ratio-Loss Correlation

The distortion-descriptor elements given can be related to the loss of compressor stability pressure ratio, as shown in Equation 24 with total-temperature distortion elements.

$$\Delta PRS = \sum_{i=1}^{N} \left[KTC_i \left(\frac{\Delta TC}{T}\right)_i + KTR_i \left(\frac{\Delta TR}{T}\right)_i + CT_i \right] \times 100 \quad \text{(Eq. 24)}$$

where:

ΔPRS = loss of stability pressure ratio due to total-temperature distortion, expressed as a percent of the undistorted stability pressure ratio

N = number of instrumentation rings

KTC_i = circumferential total-temperature distortion sensitivity of ring i (empirically determined)

KTR_i = radial total-temperature distortion sensitivity of ring i (empirically determined)

$(\Delta TC/T)_i$ = circumferential total-temperature distortion intensity of ring i, defined in 6.3.2.1

$(\Delta TR/T)_i$ = radial total-temperature distortion intensity of ring i, defined in 6.3.2.2

CT_i = offset term for ring i (empirically determined)

The sensitivity and offset coefficients will vary with the type of distortion (extent, multiple-per-rev, etc.), compression system design, and operating conditions. These coefficients are derived from test data and should be of sufficient accuracy to correlate the effect of critical distortion patterns to within ±2% of the stability pressure ratio. The loss in stability pressure ratio for downstream compression components should be calculated accordingly through the introduction of total-temperature-distortion transfer coefficients.

6.3.2 Spatial Total-Temperature Distortion Elements

Inlet spatial total-temperature distortion is described in terms of the circumferential and radial elements. These sections summarize the calculations of the distortion descriptors and the use of these descriptors in determining the stability margin for an engine.

In addition, the method for evaluating total-temperature ramp distortion is described, along with that for combined spatial total-temperature distortion and total-temperature-ramp distortion. More information about total-temperature distortion can be found in AIR5867.

a. Circumferential Distortion Elements: Circumferential distortion is described in terms of intensity, extent, and multiple-per-revolution elements.

b. Intensity: The circumferential distortion intensity (ΔTC/T) describes the magnitude of the total-temperature rise above the average for each ring.

c. Extent: The circumferential distortion extent element for each ring (θ^+) is the angular region, in degrees, in which the total temperature is above the ring-average total temperature.

d. Multiple-per-Revolution: The circumferential distortion multiple-per-revolution element (MPR) describes the number of high total-temperature regions for each ring.

e. Radial Distortion Element: The radial distortion intensity element (ΔTR/T) describes the difference between the ring-average total temperature and the face-average total temperature for each ring. Both positive and negative values of radial intensity are considered. Positive values reflect ring-average total temperature that is above the face-average total temperature.

f. Total-Temperature Ramps: Total-temperature ramps are characterized by a rapid increase or decrease in the face-average total temperature at the AIP. They can be caused by armament/exhaust gas or catapult steam ingestion, for example.

6.3.2.1 Circumferential-Distortion Elements

Circumferential distortion is described on a ring-by-ring basis in terms of intensity, extent, and multiple-per-revolution elements. The intensity or level of distortion is a numerical indication of the magnitude of the total-temperature distortion. The extent element is a numerical indication of the circumferential size of the high total-temperature region. The multiple-per-revolution element is a numerical indication of the equivalent number of circumferential regions of high total temperature.

6.3.2.1.1 One-Per-Rev Patterns

The “intensity” and “extent” elements of circumferential distortion are obtained by linear interpolation of the total temperatures in a given instrumentation ring. Example total temperatures for the probes in the i-th ring for a one-per-revolution pattern (one high total-temperature region in 360 degrees) are shown in Figure 6. Theta plus, θ_i^+, is the circumferential extent of the high total-temperature region in ring i. It is defined by the intersection between the ring-average total temperature (TAV_i) and the linear interpolation which subtends the high total-temperature region.

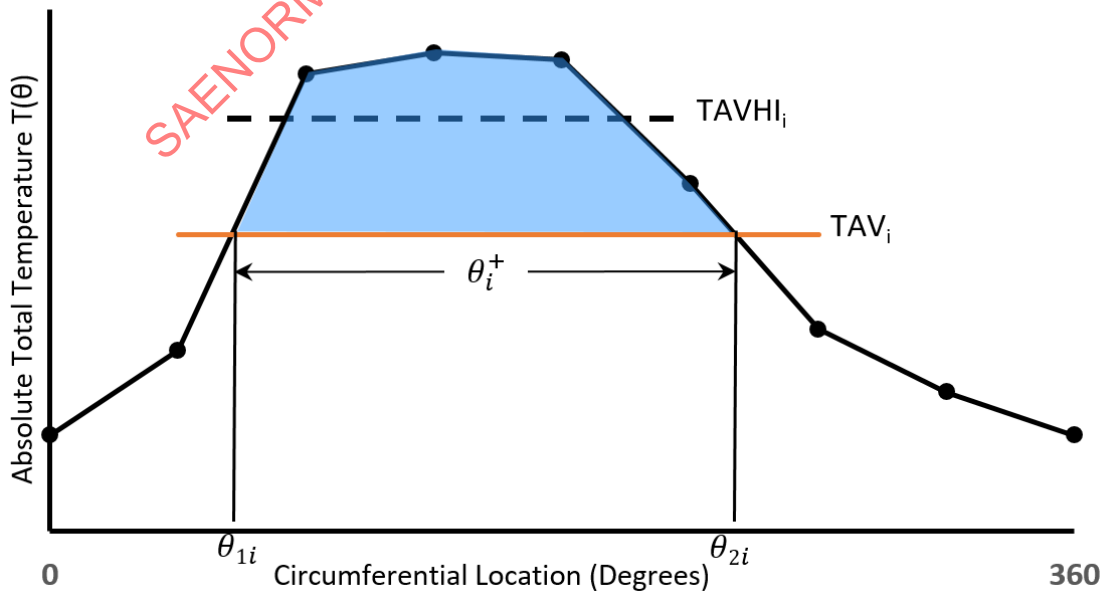

Figure 6 - Ring circumferential distortion for a one-per-rev pattern

$$\text{Extent: } \theta_i^+ = \theta_{2i} - \theta_{1i} \quad \text{(Eq. 25)}$$

$$\text{Intensity: } \left(\frac{\Delta TC}{T}\right)_i = \frac{TAVHI_i - TAV_i}{TAV_i} \quad \text{(Eq. 26)}$$

where:

$$\text{Ring Average Total Temperature: } TAV_i = \frac{1}{360}\int_0^{360} T(\theta)_i \, d\theta \quad \text{(Eq. 27)}$$

$T(\theta)_i$ is a function resulting from a linear fit between the data points.

$$TAVHI_i = \frac{1}{\theta_i^+}\int_{\theta_i^+} T(\theta)_i \, d\theta \quad \text{(Eq. 28)}$$

$$\text{Multiple-Per-Rev: } MPR_i = 1 \quad \text{(Eq. 29)}$$

6.3.2.1.2 Multiple-Per-Rev Patterns

The circumferential-distortion intensity and extent elements for multiple-per-revolution distortion patterns are also determined by a linear interpolation procedure. A pattern with two high total-temperature regions relative to the ring average separated by two low total-temperature regions of extents θ_{i1}^- and θ_{i2}^- is shown in Figure 7. In all that follows, the analytical expressions will be written for the k-th high total-temperature region for Q high total-temperature regions per ring. The extent and intensity elements of each high total-temperature region are calculated using Equations 25 and 26.

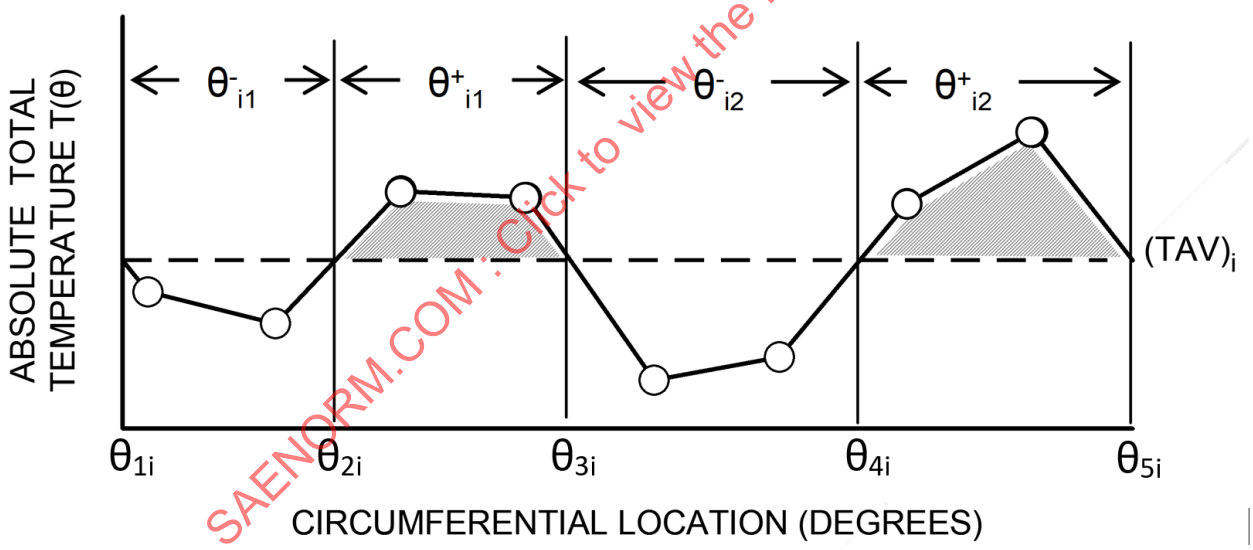

Figure 7 - Ring circumferential distortion for a multiple-per-rev pattern

6.3.2.1.2.1 Patterns with $\theta_{ik}^- \leq \theta_{min}^-$

If the pattern has high total-temperature regions circumferentially separated by low total-temperature regions with extents less than or equal to θ_{min}^-, it is considered as an equivalent one-per-revolution high total-temperature region and the multiple-per-revolution element is one. θ_{min}^- is typically specified by the engine manufacturer. A value of θ_{min}^- of 25 degrees is suggested in the absence of other information.

$$\text{Extent: } \theta_i^+ = \sum_{k=1}^{Q} \theta_{ik}^+ \quad \text{(Eq. 30)}$$

From Figure 7, $\theta_i^+ = (\theta_3 - \theta_2)_i + (\theta_5 - \theta_4)_i,$

$$\text{Intensity: } \left(\frac{\Delta TC}{T}\right)_i = \frac{TAVHI_i - TAV_i}{TAV_i} \quad \text{(Eq. 31)}$$

where:

$$TAVHI_i = \frac{1}{\theta_i^+}\sum_{k=1}^{Q}\int_{\theta_{ik}^+} T_k(\theta)_i \, d\theta \quad \text{(Eq. 32)}$$

Hence,

$$\text{Intensity: } \left(\frac{\Delta TC}{T}\right)_i = \frac{\sum_{k=1}^{Q}\left[\left(\frac{\Delta TC}{T}\right)_{ik}\theta_{ik}^+\right]}{\sum_{k=1}^{Q}\theta_{ik}^+} \quad \text{(Eq. 33)}$$

$$\text{Multiple-Per-Rev = (MPR)}_i = 1 \quad \text{(Eq. 34)}$$

6.3.2.1.2.2 Patterns with $\theta_{ik}^- > \theta_{min}^-$

If the pattern has high total-temperature regions circumferentially separated by low total-temperature regions with extents greater than θ_{min}^-, then the multiple-per-revolution element is greater than one.

Intensity $\left(\frac{\Delta TC}{T}\right)_i$ is the $\left(\frac{\Delta TC}{T}\right)_{ik}$ corresponding to the maximum value of $\left[\left(\frac{\Delta TC}{T}\right)_{ik}\theta_{ik}^+\right]$.

Extent: θ_i^+ is the θ_{ik}^+ corresponding to the maximum value of $\left[\left(\frac{\Delta TC}{T}\right)_{ik}\theta_{ik}^+\right]$.

The multiple-per-revolution term is defined as the number of equivalent high total-temperature regions, the equivalence being based on the ratio of the total integrated area above $(TAV)_i$ in Figure 7 to the largest single area above $(TAV)_i$. This is given by the equation:

$$\text{Multiple-Per-Rev: } MPR_i = \frac{\sum_{k=1}^{Q}\left[\left(\frac{\Delta TC}{T}\right)_{ik}\theta_{ik}^+\right]}{max\left[\left(\frac{\Delta TC}{T}\right)_{ik}\theta_{ik}^+\right]} \quad \text{(Eq. 35)}$$

6.3.2.2 Radial Distortion Elements

The radial distortion intensity of a ring is defined as the difference between the ring-average total temperature and the face-average total temperature, divided by the face-average total temperature. Both positive and negative values of radial intensity are considered; positive values reflect a ring average total temperature that is above the face average. A typical hub-radial distortion pattern is shown in Figure 8. The arrow indicates the difference in radial total temperature for ring 1. For the general ring, i, the radial intensity is given as

$$\text{Intensity: } \left(\frac{\Delta TR}{T}\right)_i = \frac{TAV_i - TFAV}{TFAV} \quad \text{(Eq. 36)}$$

where:

TFAV = area-weighted face-average total temperature

For rings at centers of equal area,

$$TFAV = \frac{1}{N}\sum_{i=1}^{N} TAV_i \quad \text{(Eq. 37)}$$

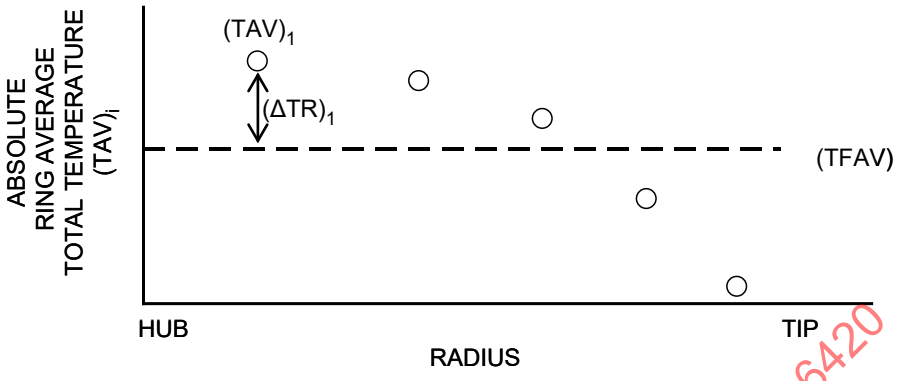

Figure 8 - Hub radial distortion pattern

6.3.3 Total-Temperature Distortion Scaling Guidelines

Total-temperature distortion scaling guidelines are presented in Table 1 for four cases ranging from where buoyancy effects predominate to a condition where momentum effects predominate. These cases are:

- Case 1 - Buoyancy-Flux Similitude Predominates over Exhaust-Exit-Mach-Number Similitude
- Case 2 - Buoyancy-Flux Similitude Predominates over Exhaust-Exit-Mach-Number Similitude where Exact Density Scaling Cannot Be Achieved
- Case 3 - Exhaust-Mach-Number Similarity Predominates over Buoyancy-Flux Similarity (Near Field and Highly-Choked Full-Scale Exhaust Nozzle) for Situations where Exact Density Scaling Cannot Be Achieved
- Case 4 - Exhaust-Mach-Number Similarity Predominates over Buoyancy-Flux Similarity (Near Field and High Exhaust Mach Numbers)

The scaling relations for velocity, total temperature, frequency, and time ratios for each of the above four cases are presented in Table 1. Additional information can be found in AIR5867.

Table 1 - Similitude ratios

Case No.	Ratios			
	Velocity	Total temperature	Frequency	Time
1	$\frac{U_{a,m}}{U_{a,f}} = \frac{U_{e,m}}{U_{e,f}} = \frac{U_{i,m}}{U_{i,f}} = \left(\frac{l_m}{l_f}\right)^{1/2}$	$\left(T_{0,A} - T_{0,a}\right)_f = \frac{\left(T_{0,e} - T_{0,a}\right)_f}{\left(T_{0,e} - T_{0,a}\right)_m}\left(T_{0,A} - T_{0,a}\right)_m$	$\frac{f_f}{f_m} = \left(\frac{l_m}{l_f}\right)^{1/2}$	$\frac{t_f}{t_m} = \left(\frac{l_f}{l_m}\right)^{1/2}$
2	$\frac{U_{a,m}}{U_{a,f}} = \frac{U_{i,m}}{U_{i,f}} = \left[\frac{(\rho_e - \rho_a)_m}{(\rho_e - \rho_a)_f}\frac{(\rho_e\rho_a)_f^{1/2}}{(\rho_e\rho_a)_m^{1/2}}\frac{l_m}{l_f}\right]^{1/2}$	$\left(T_{0,A} - T_{0,a}\right)_f \approx \frac{(\rho_a/\rho_e)_m^{1/2}}{(\rho_a/\rho_e)_f^{1/2}}\frac{\left(T_{0,e} - T_{0,a}\right)_f}{\left(T_{0,e} - T_{0,a}\right)_m}\left(T_{0,A} - T_{0,a}\right)_m$	$\frac{f_f}{f_m} = \frac{l_m}{l_f}\left(\frac{U_{a,f}}{U_{a,m}}\right)$	$\frac{t_f}{t_m} = \frac{l_f}{l_m}\left(\frac{U_{a,m}}{U_{a,f}}\right)$
3	$\frac{U_{a,m}}{U_{a,f}} = \frac{U_{e,m}}{U_{e,f}} = \frac{U_{i,m}}{U_{i,f}} = \left(\frac{T_{a,m}}{T_{a,f}}\right)^{1/2}$	$\left(T_{0,A} - T_{0,a}\right)_f \approx \frac{(\rho_a/\rho_e)_m^{1/2}}{(\rho_a/\rho_e)_f^{1/2}}\frac{\left(T_{0,e} - T_{0,a}\right)_f}{\left(T_{0,e} - T_{0,a}\right)_m}\left(T_{0,A} - T_{0,a}\right)_m$	$\frac{f_f}{f_m} = \frac{l_m U_f}{l_f U_m} = \frac{l_m}{l_f}\left(\frac{T_{a,f}}{T_{a,m}}\right)^{1/2}$	$\frac{t_f}{t_m} = \frac{l_f}{l_m}\left(\frac{T_{a,m}}{T_{a,f}}\right)^{1/2}$
4	$\frac{U_{a,m}}{U_{a,f}} = \frac{U_{e,m}}{U_{e,f}} = \frac{U_{i,m}}{U_{i,f}} = \left(\frac{T_{a,m}}{T_{a,f}}\right)^{1/2}$	$\left(T_{0,A} - T_{0,a}\right)_f = \frac{\left(T_{0,e} - T_{0,a}\right)_f}{\left(T_{0,e} - T_{0,a}\right)_m}\left(T_{0,A} - T_{0,a}\right)_m$	$\frac{f_f}{f_m} = \frac{l_m U_f}{l_f U_m} = \frac{l_m}{l_f}\left(\frac{T_{a,f}}{T_{a,m}}\right)^{1/2}$	$\frac{t_f}{t_m} = \frac{l_f}{l_m}\left(\frac{T_{a,m}}{T_{a,f}}\right)^{1/2}$

6.3.4 Total-Temperature-Ramp Distortion Methodology

The basis for the methodology outlined above to analyze spatial total-temperature distortion is the assumption that total-temperature distortion can be handled in a manner similar to total-pressure distortion. The data available to evaluate the applicability of this method substantiate this assumption, as explained in AIR5867. An example which can be used to understand engine response to total-temperature ramps and assess combined effects of spatial total-temperature distortion and a total-temperature ramp is described in AIR5867.

The procedure for assessing the stability margin loss caused by combined spatial total-temperature distortion and total-temperature ramps should account for both engine operating-line and the engine stability-limit-line responses. The shift in the engine operating line is dominantly caused by the total-temperature ramp (change in the average inlet total temperature per unit time). The shift in the engine stability limit line is caused by temperature induced changes in compressor stage matching and variable geometry mis-schedule. These factors are influenced by both spatial total-temperature distortion (analogous to spatial total-pressure distortion) and total-temperature ramps. The effect of spatial total-temperature distortion on the engine stability limit line can be calculated using the descriptors and methodology (ΔPRS) defined in 6.3.1. The loss of stability margin caused by a total-temperature ramp can be assessed using compression system and engine transient models. The method also assumes that the loss of engine stability margin due to spatial total-temperature distortion and total-temperature ramps can be combined.

Time-variant readings of a set of total-temperature probes are measured at the AIP. Probe readings are corrected for probe response time constant. A sequence of time slices is analyzed. For each time slice, the difference between individual probe readings and an area-weighted average is used to calculate distortion elements and/or descriptors (6.3.2) which are used in empirical formulae to estimate the loss in stability pressure ratio due to spatial total-temperature distortion. The time-variation of the area-weighted average of the AIP readings describes a total-temperature ramp.

There is a significant corrected airflow excursion associated with a total-temperature ramp (Figure 9). Consequently, the ramp is analyzed in a sequence of time slices in which the instantaneous distortion is used to degrade the stability limit line and an engine dynamic simulation is used to evaluate the transient operating line. The residual stability margin is evaluated over the airflow excursion caused by the total-temperature ramp and a stability assessment is made at the pinch point where the residual stability margin is minimal.

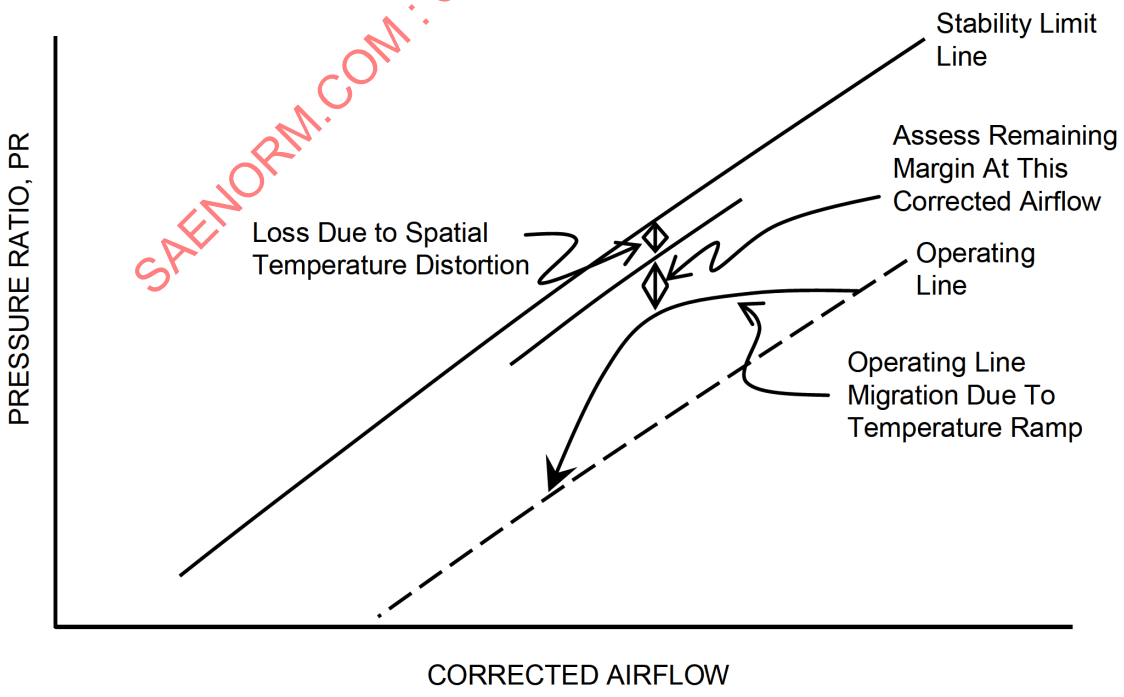

Figure 9 - Compressor map characteristics with total-temperature distortion

6.4 Swirl Distortion

Swirl-distortion methodology has not been developed to the point where there is consensus among all interested parties and thus is not included in this document. The following paragraphs provides a brief description of the characteristics of inlet distortion due to swirl along with a reference for additional information.

Inlet-flow swirl distortion is a measure of the variation of the circumferential portion of the flow velocity vector at the AIP. It is characterized in terms of the swirl angle, which is the circumferential angle between an axial vector and the actual flow velocity vector. The swirl-distortion pattern is representative of the distribution of swirl angle over the AIP.

Many embedded installations of gas turbines are supplied with air through inlet systems that involve one or more tight turns leading up to the compressor. These inlet systems can generate swirl distortion in all operating conditions. Some applications with strong crossflows such as lift fans in forward flight will experience swirl distortion during transition operations. A detailed discussion of sources of swirl distortion at the AIP station of a compressor, along with a proposed methodology, is presented in AIR5686. AIR5686 can be consulted to determine whether swirl is likely to have an impact on operability and performance.

7. THE AERODYNAMIC INTERFACE PLANE GUIDELINES

The Aerodynamic Interface Plane (AIP) is an interface mutually agreed upon between the airframer, the engine manufacturer, and the procuring agency/company. The AIP probe and rake arrangement should remain invariant throughout the life cycle of the propulsion system. The AIP identifies the location at which the inlet system aerodynamic characteristics are quantified for use by the engine manufacturer.

The AIP is also the location where a mutually-agreed-upon set of instrumentation is defined. The type of instrumentation required (steady-state total-pressure probes, dynamic total-pressure probes, static-pressure probes, flow-angularity probes, total-temperature probes, etc.) and number of probes are determined by the expected inlet flow field, the engine geometry and number of engine flow streams, the aerodynamic flow characteristics to be measured, and the space available to fit the instrumentation while minimizing the effect on the aerodynamic flow characteristics.

The AIP should be located in a round or annular section of the inlet/engine face located as near as possible to the engine face. All the flow and only the flow that enters the engine should pass through the AIP. The AIP should be located so that the effects of all inlet features, such as auxiliary inlet flow, are measured by the instrumentation suite. Rake and probe locations and orientations should be consistent between subscale and full-scale test articles. Location of a rake at top dead center (TDC), as shown in Figure 10, is not a requirement. Pre-test flow analysis and aircraft structural features should guide selection of appropriate axial and circumferential positions for the probes at the AIP.

7.1 AIP Rake Considerations for Total-Pressure and Planar-Wave Distortion

The AIP rake array should be designed to capture the flow physics to be measured. The recommended minimum arrangement of measurement probes at the AIP is shown in Figure 10. If the probes are not located at centers of equal area, calculations must be area-weighted. Where there are outer annular flow streams upstream of the fan, a minimum of two additional rings should be placed in each annular flow stream. To accurately capture unique flow field effects, the number of rakes and probes and the spacing of individual rakes and probes can be adjusted with coordinated agreement between the inlet designer and engine manufacturer.

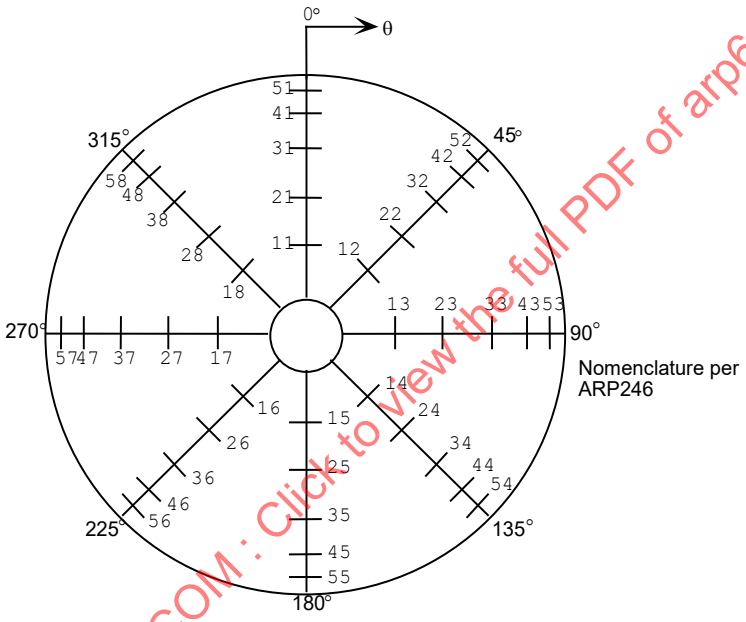

Figure 10 - Probe orientation - view aft looking forward

An equation to calculate the radii of the rings on centers of equal area is:

$$R(i) = \sqrt{R_{in}^2 + \left(\frac{R_{out}^2 - R_{in}^2}{N}\right)\left(\frac{2i-1}{2}\right)} \quad \text{(Eq. 38)}$$

where:

R_{in} = inner radius

R_{out} = outer radius

N = number of rings

i = ring number

For the case with no hub ($R_{in} = 0$), the above equation simplifies to:

$$R(i) = \sqrt{\left(\frac{R_{out}^2}{N}\right)\left(\frac{2i-1}{2}\right)} \quad \text{(Eq. 39)}$$